Vol. 15, No. 42, Spring 2025, Pages 15-23

Journal of Analytical and Numerical Methods in Mining Engineering

Journal home page: http://anm.yazd.ac.ir/

Research article

Joint Interpretation of Electromagnetic in Low Induction Number and Electrical Resistivity Tomography: A Case Study on Data From an Area in South Africa

Hosseinali Ghari[1*]

1- Dept. of Mining and Metallurgy Engineering, Yazd University, Yazd, Iran

(Received: *September 2023*, Accepted: *June 2024*)

DOI: *10.22034/ANM.2024.20684.1610*

Keywords

ERT
EM-LIN
Joint interpretation
Inversion
South Africa

English Extended Abstract

Summary

Quantitative interpretation of electrical resistivity tomography (ERT) and electromagnetic in low induction number (EM-LIN) data sets is possible through inversion. Data inversion of the two methods is confronted with two problems of non-uniqueness and instability, which must be solved by the use of constraints and a priori information. The more important issue is that the implementation of one geophysical method does not lead to a favorable interpretation of the subsurface structure in many cases, so the combination of geophysical data is inevitable. In this paper, the joint interpretation of resistivity and electromagnetic data in low induction number data is used for a site in South Africa. In this area, the identification of dolerite dyke is the most important goal in the exploration of underground water. Here, a 2D forward modeling code for EM-LIN and ERT is developed based on the integral equation (IE) method. Also, a linear relation between model parameters and apparent conductivity values is proposed. To invert both data sets, the weighted minimum length solution algorithm is used, and the depth weighting function is used as the model weighting matrix. The inversion of electromagnetic in low induction number indicates a relatively thick dyke in the depth range of less than 5 to 15 m and with a horizontal extension of 185 to 200 m (thickness is about 15 m). Electrical resistivity tomography recovers a two layered medium, and in the conductive layer close to the surface of the dyke, a resistive dyke is extended to near the surface. The electromagnetic method reconstructs the dyke better, while electrical resistivity tomography can recover the layered structure.

Introduction

Interpretation of ERT and electromagnetic data requires inverse modeling because direct interpretation of measured data is not possible except for very simple cases, and this can be accomplished qualitatively. Furthermore, unlike seism methods for which data processing provides sufficient information for interpretation, there is no efficient technique available for quantitative interpretation of ERT and electromagnetic data. Individual data inversion has provided successful interpretations of subsurface anomalies for decades [1-4], but there are many cases where individual inversion does not result in a high-resolution image of the subsurface. As a result, a combination of geophysical methods is very important, which may be done in three general ways: 1) joint interpretation [5], 2) sequential or cooperative inversion [6], and 3) joint inversion [7]. In the joint interpretation, the inversion of each method is obtained separately, then the final model of the subsurface is presented based on the inversion models, geological information, and the available a priori information. In this paper, the joint interpretation of ERT and EM-LIN data is used for the site in South Africa. The dolerite dyke in this area is the main anomaly for groundwater exploration.

*Corresponding author: E-mail: *hosseinali.ghari@gmail.com*

Vol. 15, No. 42, Spring 2025, Pages 15-23

Journal of Analytical and Numerical Methods in Mining Engineering

Journal home page: http://anm.yazd.ac.ir/

Methodology and Approaches

Perez-Flores et. al introduced linear IEs for 3D EM-LIN modeling of horizontal and vertical magnetic dipoles using the Born approximation [8]. These IEs are Fredholm Integral equations of the first kind for which observed apparent resistivities are linearly related to the true conductivities as follows: equations for vertical magnetic dipoles (VMD) [11]:

$$\sigma_a(r_1, r_2) = -\frac{16\pi s}{\omega\mu_0 m_z}\iint_v G_{Hz}(r, r_2).E_{Hz}(r, r_1)\sigma(r)d^3r \tag{1}$$

and for horizontal magnetic dipoles (HMD):

$$\sigma_a(r_1, r_2) = -\frac{16\pi s}{\omega\mu_0 m_y}\iint_v G_{Hy}(r, r_2).E_{Hy}(r, r_1)\sigma(r)d^3r \tag{2}$$

where s, ω and μ_0 stand in turn for T-R separation, angular frequency, and magnetic permeability, while m_z and m_y are a magnetic momentum around the z and y directions, respectively. σ_a and σ(r) express observed apparent conductivity and conductivity distribution of the subsurface. r_1, r_2 and r represent position vectors of the transmitter, receiver, and subsurface model, respectively. To obtain appropriate expressions for the corresponding 2D problem, we integrate equations (1) and (2) from minus infinity to infinity along the y-axis (strike direction), which can be made analytically or numerically. In this paper, numerical integration is made to achieve the 2D case. Therefore, by implementing numerical integration along the y-axis, we may form the following matrix equations for each configuration of magnetic dipoles:

$$d_E = A_E m_E \tag{3}$$

where dE is the vector of measured apparent resistivities, mE contains unknowns (model parameters), and AE is the kernel matrix or forward operator.

In fact, ERT forward problem can be considered as a Fred-Holm Integral Equation of the first kind whose 2D form of can be written as [9]:

$$d(s) = \int G(s.x_c.z_c)m(x_c.z_c)dxdz \tag{4}$$

s stands for current and potential electrodes, d refers the logarithm of apparent resistivity values, (x_c.z_c) are coordinates of points of the interested area, G is kernel and m is the model.

Like EM-LIN method, the following matrix equation can be obtained from the discretization of equation (4):

$$d_R = A_R m_R \tag{5}$$

AR is the 2D forward operator, dR is data vector and mR refers to the model.

Since both inverse problems are linear, therefore following damped weighted minimum length solution algorithm is utilized for the inversion process [9]:

$$m = m_a + (W_m A^T A + \alpha^2 I)^{-1}(W_m A^T)(d - Am_a) \tag{6}$$

I and α are the identity matrix and the regularization parameter, respectively. W_m representing depth weighting matrix is defined as [10]

$$W_m = \frac{1}{{z_c}^{\beta}} \tag{7}$$

z_c is the z coordinate of cell centers, and β is the depth weighting exponent.

Vol. 15, No. 42, Spring 2025, Pages 15-23

Journal of Analytical and Numerical Methods in Mining Engineering

Journal home page: http://anm.yazd.ac.ir/

Results and Conclusions

Using the presented algorithm, the results of EM-LIN data inversion for both vertical magnetic dipole (VD) and horizontal magnetic dipole (HD) configurations are shown in Figure 1. These models represent high consistency. Conductivity models indicate a dyke in the horizontal range of 185 to 200 meters. Also, the depth range of the dyke is from less than 5 meters to about 15 meters. In addition, it should be noted that the section of the VD arrangement is somewhat noisy. The curves of calculated data versus measured data for both arrangements are depicted in Figure 2. Computed data fitting is better for the arrangement with horizontal dipoles.

The resistivity cross-section recovered from the inversion of the data indicates an almost two-layered earth, where the first layer is more conductive. In the middle of the conductive layer, a resistive anomaly has extended to near the surface, which shows the compatibility of the results of both ERT and EM-LIN methods. The pseudo-sections of measured data and calculated data can be seen in Figure 3.

In order to have a better comparison of the obtained models of both methods, we convert the conductivity cross-sections of the EM-LIN into resistivity cross-sections. This issue is easily possible considering that the resistivity=1/conductivity. Indeed, the inversion section of ERT data is displayed only up to a depth of 25 meters (Figure 4), allowing easy comparison. Comparing of these sections clearly shows the higher resolution of the electromagnetic method in the reconstruction of dyke model, while the ERT method represents the layered structure below the surface.

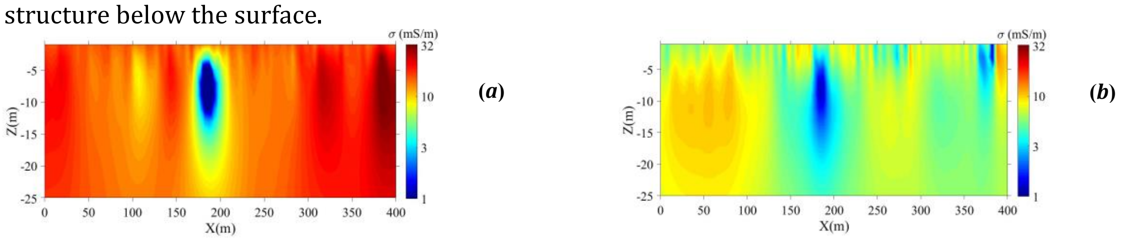

Fig 1. (a)Conductivity model obtained by inversion of EM-LIN data for the HD array and (b) Conductivity model obtained by inversion of EM-LIN data for the VD array.

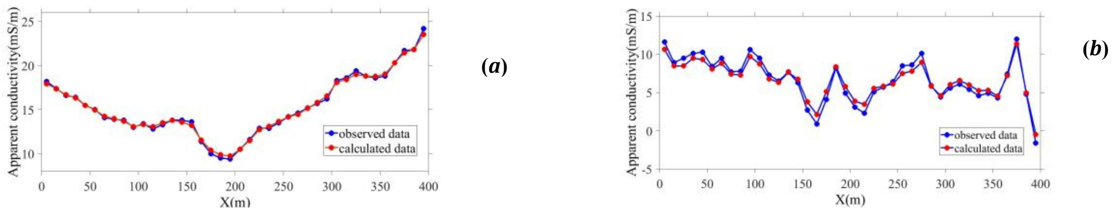

Fig 2. Comparison between observed apparent electrical conductivity for EM-LIN data and predicted data from inverted models: a) HD array and b) VD array.

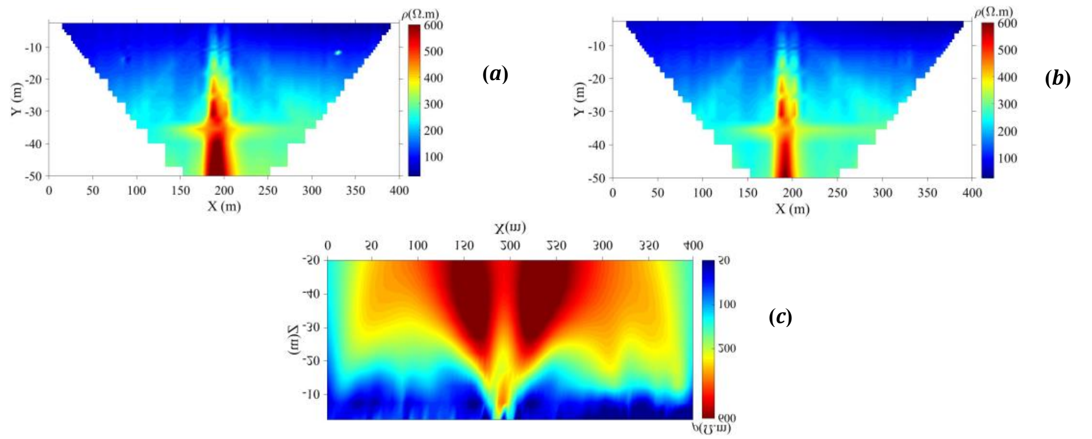

Fig 3. a) The pseudo-section of ERT measured data, b) The pseudo-section of ERT calculated data, and c) The section obtained by inversion of ERT data.

*Corresponding author: E-mail: hosseinali.ghari@gmail.com

Vol. 15, No. 42, Spring 2025, Pages 15-23

Journal of Analytical and Numerical Methods in Mining Engineering

Journal home page: http://anm.yazd.ac.ir/

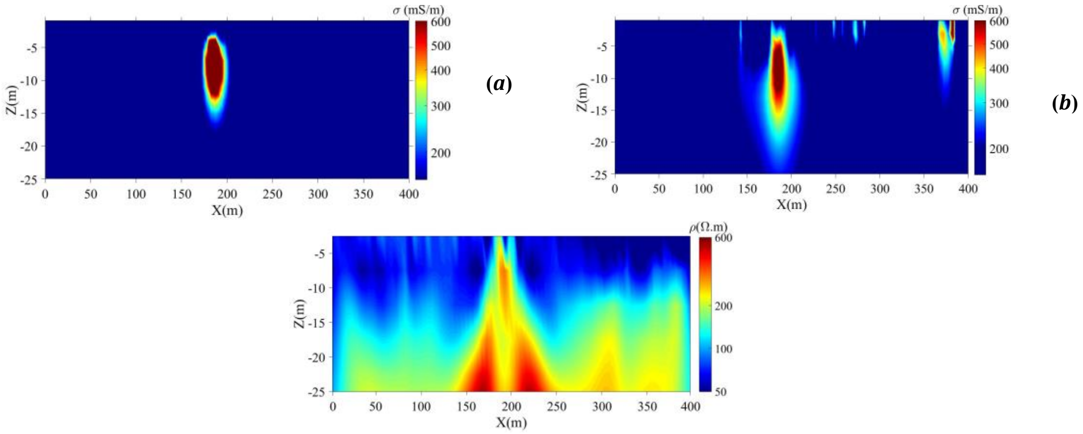

(c)

Fig 4. (a) Resistivity model obtained by inversion of EM-LIN data for the HD array, (b) Resistivity model obtained by inversion of EM-LIN data for the VD array, and (c) Resistivity model obtained by inversion of ERT data.

References

[1] Loke, M. H., and Barker, R. D. (1996). Rapid least-squares inversion of apparent resistivity pseudo-sections by a quasi-Newton method. Geophysical prospecting 44(1), 131-152.

[2] Cella, F. and Fedi, M. (2012). Inversion of potential field data using the structural index as weighting function rate decay. Geophysical Prospecting 60 (2), 313-336.

[3] Ghari, H. A., Voge, Malte., Bastani, M., Pfaffhuber, A. A., and Oskooi, B. (2020). Comparing resistivity models from 2D and 1D inversion of frequency domain HEM data over rough terrains: cases study from Iran and Norway. Exploration Geophysics 51(1), 45-65.

[4] Ghari, H., Oskooi, B., and Bastani (2020). M. Multi-Line 1D Inversion of Frequency-Domain Helicopter-Borne Electromagnetic Data with Weighted 3D Smoothness Regularization: A Case Study from Northern Iran. Pure and Applied Geophysics 177, 5299–5323 .

[5] Ghari, H., Varfinezhad, R., and Parnow, S. (2023). 3D joint interpretation of potential field, geology, and well data to evaluate a salt dome in the Qarah-Aghaje area, Zanjan, NW Iran. Near Surface Geophysics 21(3), 233-246.

[6] Varfinezhad, R., Parnow, S., Florio, G., Fedi, M., & Mohammadi Vizheh, M. (2023). DC resistivity inversion constrained by magnetic method through sequential inversion. *Acta Geophysica*, *71*(1), 247-260.

[7] Gallardo, L. A., & Meju, M. A. (2004). Joint two-dimensional DC resistivity and seismic travel time inversion with cross-gradients constraints. *Journal of Geophysical Research: Solid Earth*, *109*(B3).

[8] Pérez-Flores, M. A., Méndez-Delgado, S., & Gómez-Treviño, E. (2001). Imaging low-frequency and dc electromagnetic fields using a simple linear approximation. Geophysics, 66(4), 1067-1081.

[9] Varfinezhad, R., Ghari, H., and Rafiei, R. (2022). Topography incorporated inversion of DC resistivity data using integral equation vs. Res2dinv software. Bulletin of Geophysics and Oceanography 63(3), 427-442.

[10] Li, Y., & Oldenburg, D. W. (1996). 3-D inversion of magnetic data. Geophysics, 61(2), 394-408.

[11] Ghari, H., & Varfinezhad, R. (2022). 2D Linear inversion of ground-based controlled-source electromagnetic data under a low induction number condition. Journal of the Earth and Space Physics 48(3), 557-573 (In Persian).